




# Influence of surfactants on the electrospinnability of lignin-PVP solutions and subsequent oil structuring properties of nanofiber mats

M. Borrego<sup>1</sup> · J. E. Martín-Alfonso<sup>1</sup> · C. Valencia<sup>1</sup> · M. C. Sánchez<sup>1</sup> · J. M. Franco<sup>1</sup> 

Received: 20 April 2022 / Revised: 27 June 2022 / Accepted: 13 July 2022  
© The Author(s) 2022

## Abstract

This work focuses on the improvement of the electrospinnability of low-sulfonate lignin (LSL)/polyvinylpyrrolidone (PVP) solutions by the addition of surfactants (SDS, CTAB and Tween-20) as well as on the ability of resulting nanofibers to structure castor oil. Solutions with two LSL/PVP weight ratios (70:30 and 90:10) in DMF were prepared by adding variable surfactant concentrations (0–1 wt.%), and physicochemically characterized. Electrical conductivity, surface tension and rheological measurements were performed. Variations of these physicochemical properties were explained on the basis of surfactant-polymer interactions. The addition of surfactants to LSL/PVP solutions improves electrospinnability, producing more compact and uniform fiber mats in 70:30 LSL/PVP systems, generally reducing the average diameter of the nanofibers and the number of beads. In contrast, nanofiber mats were not obtained with 90:10 LSL/PVP solutions, but different nanostructures composed of particle clusters. Dispersions of nanofiber mats obtained by electrospinning from 70:30 LSL/PVP solutions in castor oil were able to generate physically stable strong oleogels. In general, linear viscoelastic functions of oleogels increased with surfactant concentration. In addition, these oleogels exhibited excellent lubrication performance in a tribological contact, with extremely low values of the friction coefficient and wear diameters, which may lead to potential applications as lubricants.

**Keywords** Electrospinning · Lignin · Lubricant · Oil structuring · Surfactant

---

✉ J. M. Franco  
franco@uhu.es

<sup>1</sup> Pro2TecS – Chemical Process and Product Technology Research Center, Department of Chemical Engineering and Materials Science. ETSI, Universidad de Huelva, Campus de “El Carmen”. 21071, Huelva, Spain

## Introduction

Nowadays, there is a growing interest in exploiting waste materials and by-products to manufacture end-use products and thus reduce resource depletion and/or expensive disposal treatments [1–4]. This is the case of lignin, which is produced in huge amounts in the paper industry where is considered a waste or low valuable by-product, and whose main use consists of direct incineration to recover some of the energy spent during the process [5, 6]. So far, the valorization of lignin as raw material in added-value products is scarcely explored, probably due to its complex chemical nature and the variability of its composition and structure. However, this issue has recently been a matter of intensive research [7, 8] and, nowadays, lignin is considered a renewable resource with great potential for different industrial applications [9].

On the other hand, the development of bio-based oleogels from renewable raw materials represents a target for the lubricant industry to mitigate the well-known environmental problems associated with lubricant spillage [10]. In previous research, the Chemical Process and Product Technology Research Center (Pro-2TecS, University of Huelva) has dedicated great efforts to develop eco-friendly oleogels, attempting to mimic the functional properties of traditional lubricating greases [11, 12]. Among the different biopolymers tested as oil thickening agents, lignins were found to be a promising alternative upon chemical modifications, such as epoxidation [13, 14] or isocyanate functionalization [15–17], that promote the formation of chemical gels by generating covalent bonds between lignin and vegetable oil. However, despite the fact that these final formulations may be considered bio-based, inert, and non-toxic materials, some of these chemical modifications involve the use of non-green chemicals and solvents and, therefore, alternative cleaner processes and methodologies must be further explored. In a previous work [18], the electrospinning technique was employed to produce lignin nanofibers with the ability to physically structure vegetable oils by simply dispersing the electrospun nanofiber mats in the oil, thus avoiding previous complex chemical functionalization. This procedure results in a much simpler and green strategy to produce oleogels. However, to obtain appropriate nanofiber morphologies, lignin must be doped with a readily electrospinnable polymer such as PVP. Besides, in general, the lignin electrospinning process still has room for improvement, for instance by optimizing the physicochemical properties of the solution to be electrospun.

The addition of surfactants to polymer solutions has been a common practice to improve electrospinnability, mainly due to a drastic reduction of the surface tension, but also to the modification of other important physicochemical properties such as viscosity and electrical conductivity. The change in these properties depends on the nature of the polymer and the surfactant that govern the interactions between them. For instance, Kumar and Tyagi [19] studied the interactions between PVP and anionic surfactants, such as SDS and a carboxylate-based dimeric surfactant. Different conformations of the PVP-surfactant complexes were proposed depending on the surfactant concentration ranges, delimited by

the critical aggregation concentration (CAC) and the critical micellar concentration (CMC), respectively. The CAC was defined as the surfactant concentration required for the onset of the interaction between the surfactant and the polymer. These authors also proposed simple experimental methods to determine these critical concentrations through conductometric and surface tensiometric measurements. On the other hand, Wang et al. [20] observed a considerable increment in the viscosity of PEG/surfactant solutions which they associated with the formation of transient polymer networks crosslinked by surfactant micelles.

In direct relation with the improvement of electrospinnability, Jia et al. [21] and Fang et al. [22] studied polymer-surfactant interactions in PVA and lignin/PVA solutions, respectively, and how these interactions influence the physicochemical properties of the solution depending on the nature of both the polymer and the surfactant. Jia et al. [21] concluded that, apart from the beneficial effect of decreasing the surface tension, the solution viscosity steadily increased with the concentration of ionic surfactants, which was attributed to the formation of PVA-surfactant complexes, while non-ionic or amphoteric surfactants did not significantly affect the solution viscosity. In the presence of lignin, Fang et al. [22] also attributed the increase in viscosity to the formation of complexes after exceeding a critical surfactant concentration, depending on the type of surfactant. This increase was especially relevant in the case of SDS. However, they obtained a decrease in viscosity with cationic and non-ionic surfactants due to favorable electrostatic forces or the absence of cooperative binding among the complexes. Araujo et al. [23] investigated the improvement of the electrospinnability of PVA solutions by reducing the surface tension upon the addition of a non-ionic surfactant, reporting an important reduction of beads in the nanofiber mats as surfactant concentration increased, finally yielding almost bead-free nanofibers at high surfactant concentration. Similarly, Kriegel et al. [24] concluded that the addition of surfactants to PEO/chitosan solutions induced an improvement in membrane morphology, decreasing the bead content. The solution properties were especially affected by the interaction of ionic surfactants and chitosan, which is a polycationic polymer. In the same line, Wang et al. [25] reported a significant decrease in the nanofiber width by adding a non-ionic surfactant to electrospun PVP solutions.

In this work, the addition of surfactants to lignin/PVP solutions was studied aiming to improve electrospinnability and reduce heterogeneity and the appearance of defects and beads in the morphology of nanofibers. Further, how this morphology affects the ability of nanofiber mats to structure castor oil was investigated as well as the potential use of resulting oleogels as lubricants by analyzing their rheological and tribological properties.

## Experimental

### Materials

Low sulfonate Kraft lignin (LSL,  $M_w$ :~10,000 g/mol) and polyvinylpyrrolidone (PVP,  $M_w$ :~360,000 g/mol) were obtained from Merck Sigma-Aldrich. *N*,

*N*-Dimethylformamide (DMF, purity  $\geq 99.8\%$ ) was used as solvent to prepare LSL/PVP solutions. Sodium dodecyl sulfate (SDS), hexadecyltrimethylammonium bromide (CTAB) and polyethylene glycol sorbitan monolaurate (Tween-20) were used as anionic, cationic and non-ionic surfactants, respectively, in LSL/PVP solutions, all of them also purchased from Merck Sigma-Aldrich. Castor oil was supplied by Guinama (Spain), whose main physical properties and fatty acid composition can be found elsewhere [26].

### Preparation and physicochemical characterization of LSL/PVP solutions

LSL/PVP solutions in DMF were prepared at a 15 wt.% total concentration and two different LSL/PVP weight ratios (70:30 and 90:10). SDS, CTAB or Tween-20 was also added at small concentrations in the range 0–1 wt.%. The surfactant was dissolved for two hours at 50 °C in DMF under agitation. The corresponding amounts of LSL and PVP were then added while maintaining magnetic stirring for 24 h. The final solution was then centrifuged for 10 min at 3000 rpm and filtered to verify the complete dissolution.

Rheological characterization was carried out in a controlled-strain rheometer (ARES, Rheometric Scientific), in a shear rate range of 0.03–300 s<sup>-1</sup>, at 25 °C, using a Couette geometry (inner radius 16 mm, outer radius 17 mm, height 33.35 mm). LSL/PVP solutions are Newtonian for a 90:10 LSL/PVP weight ratio, whereas at a 70:30 LSL/PVP weight ratio they showed a non-Newtonian flow response which was satisfactorily fitted ( $R^2 > 0.995$ ) to the Williamson model:

$$\eta = \frac{\eta_0}{1 + (K \dot{\gamma})^m} \quad (1)$$

where  $\eta$  is the apparent viscosity,  $\dot{\gamma}$  is the shear rate,  $\eta_0$  is the zero-shear-rate-limiting viscosity, and  $m$  and  $K$  are fitting parameters.

Electrical conductivity was measured using a LAQUA PC-110 conductivity meter (Horiba Scientific) at room temperature. Surface tension was measured in a Sigma 703D tensiometer (Biolin Scientific) using a Wilhelmy platinum plate with a measuring range of 1–1000 mN/m. All measurements were replicated at least twice.

### Electrospinning process and morphological characterization of electrospun nanostructures

LSL/PVP solutions in DMF were submitted to electrospinning in a Doxa Microfluids equipment using a 10-ml BD syringe of 11.99 mm internal diameter and a flat 20G needle connected to a high voltage power source, where the negative terminal was connected to an aluminum collector plate and the positive terminal to the needle, in a horizontal configuration. The distance between needle and collector was set at 10 cm, and the feed flow and voltage applied were varied in the 0.5–1 ml/h and 17–21 kV ranges, respectively. A camera coupled to the electrospinning chamber was used to control the correct formation of the Taylor cone and detect flow instabilities. All experiments were carried out at room temperature ( $22 \pm 1$  °C).

The morphology of the nanostructures obtained by electrospinning was assessed by scanning electron microscopy (SEM) observations carried out on both the JEOL, model JXA-8200 SuperProbe, and the Hitachi, model FlexSEM 1000 II, microscopes, operating at 10–20 kV accelerating voltages and different magnifications. The open-source FIJI ImageJ analysis program was used to analyze the SEM images.

## Preparation and characterization of oleogels

LSL/PVP nanofiber templates obtained by electrospinning were dispersed in castor oil by applying agitation with an anchor geometry, at room temperature, for 24 h. The concentration of electrospun mats was fixed at 20% wt. The homogeneity of oleogel microstructure was verified with an Olympus BX51 optical microscope.

Resulting oleogels were rheologically characterized using a Rheoscope (ThermoHaake) controlled-stress rheometer and an ARES (Rheometric Scientific) controlled-strain rheometer, at 25 °C, using plate-plate geometries (25 and 35 mm diameter, respectively, and 1 mm gap). Small-amplitude oscillatory shear (SAOS) tests were performed inside the linear viscoelastic regime in a frequency range of 0.08–100 rad/s. At least two replicates of each test were performed.

Oleogels were also tribologically characterized to explore potential applications as lubricants. The tribological characterization was carried out in a tribological cell coupled to a Physica MCR-501 (Anton-Paar) controlled-stress rheometer, using a 1/2"-diameter steel ball-on-three 45°-inclined steel plates configuration. Constant axial normal load and a rotational speed of 30 N and 20 min<sup>-1</sup>, respectively, were applied for 10 min, while recording the friction coefficient values. The effective normal force on plates and friction coefficient were calculated from the applied axial normal force, the friction force measured by the rheometer and the ball radius according to Heyer and Lauger [27]. At least four replicates of each test were carried out at ambient temperature.

## Results and discussion

### Influence of surfactants on the physicochemical properties of LSL/PVP solutions.

All LSL/PVP solutions are Newtonian for a 90:10 LSL/PVP ratio, independently of the type and concentration of the surfactant. The viscosity values at 25 °C are shown in Table 1. As can be seen, the viscosity of LSL/PVP solutions initially decreased with surfactant addition and then increased from a critical concentration (~0.1 wt.%), in the case of ionic surfactants (SDS and CTAB). However, viscosity slightly decreased initially and remained almost constant when adding a non-ionic surfactant (Tween-20). Similar effects have been reported for lignin/PVA solutions in water [22], which were attributed to the different surfactant–lignin and surfactant–neutral polymer interactions. On the one hand, neutral polymers such as PVP and surfactants are able to form different kinds of associations depending on the concentration, which in turn may entail interactions between polymer chains

**Table 1** Physicochemical properties of LSL/PVP 90:10 solutions containing different types and concentrations of surfactants

Solution	Viscosity ( $\mu$ ) (Pa·s)	Electrical conductivity ( $k$ ) ( $\mu\text{S}/\text{cm}$ )	Surface tension ( $\sigma$ ) (mN/m)
90:10 LSL/PVP (surfactant-free)	$0.07 \pm 2.8 \cdot 10^{-3}$	$523.7 \pm 4.7$	$37.12 \pm 0.02$
90:10 LSL/PVP + SDS			
0.01%	$0.07 \pm 3.3 \cdot 10^{-2}$	$540.7 \pm 2.0$	$36.37 \pm 0.32$
0.05%	$0.06 \pm 4.8 \cdot 10^{-3}$	$549.7 \pm 2.1$	$34.95 \pm 0.12$
0.1%	$0.02 \pm 5.1 \cdot 10^{-2}$	$665.3 \pm 2.5$	$33.21 \pm 0.09$
0.5%	$0.06 \pm 2.7 \cdot 10^{-2}$	$984.6 \pm 2.7$	$32.75 \pm 0.11$
1%	$0.26 \pm 1.5 \cdot 10^{-1}$	$1063.6 \pm 2.3$	$30.27 \pm 0.21$
90:10 LSL/PVP + Tween-20			
0.01%	$0.06 \pm 2.1 \cdot 10^{-2}$	$516.1 \pm 1.6$	$37.19 \pm 0.08$
0.05%	$0.05 \pm 5.3 \cdot 10^{-3}$	$545.1 \pm 9.5$	$36.11 \pm 0.11$
0.1%	$0.05 \pm 1.3 \cdot 10^{-2}$	$519.3 \pm 4.04$	$32.29 \pm 0.23$
0.5%	$0.03 \pm 1.2 \cdot 10^{-2}$	$504.3 \pm 5.7$	$30.95 \pm 0.88$
1%	$0.04 \pm 6.7 \cdot 10^{-3}$	$536.4 \pm 6.8$	$30.08 \pm 1.45$
90:10 LSL/PVP + CTAB			
0.01%	$0.07 \pm 1.5 \cdot 10^{-3}$	$544.6 \pm 1.2$	$36.42 \pm 1.91$
0.05%	$0.06 \pm 9.3 \cdot 10^{-3}$	$548.0 \pm 4.6$	$34.67 \pm 0.15$
0.1%	$0.05 \pm 1.4 \cdot 10^{-2}$	$573.3 \pm 2.5$	$32.02 \pm 0.76$
0.5%	$0.08 \pm 6.4 \cdot 10^{-2}$	$672.1 \pm 1.0$	$29.49 \pm 0.31$
1%	$0.11 \pm 3.3 \cdot 10^{-3}$	$892.3 \pm 3.6$	$29.12 \pm 0.19$

and single surfactants molecules, or more complex assemblies involving surfactant aggregations and micelles [19, 20]. These associations are driven by electrical and hydrophobic interactions yielding an increase in viscosity especially in the case of ionic surfactants. For non-ionic surfactants, the cooperative binding between the surfactant and polymer is much more constrained [21]. On the other hand, the polar hydroxyl and carboxyl groups of lignin are able to interact electrostatically with ionic surfactants. Fang et al. [22] argued that the cationic surfactant interacts with lignin forming binary complexes and reducing the interaction between a neutral polymer (PVA) and both lignin and surfactant, at least up to a critical aggregation concentration, whereas the electrostatic repulsion between SDS and lignin prevents the formation of such complex but reinforces the entanglement among SDS, lignin and PVA. In general, the increase in viscosity is especially favored by the formation of surfactant–polymer complexes above a critical concentration known as critical aggregation concentration (CAC), which determine the onset of the interaction between the surfactant and the polymer.

For a lower LSL/PVP weight ratio (70:30), the solutions showed a non-Newtonian response and the viscosity always increased with surfactant concentration above 0.01 wt. %, regardless of the type of surfactant. This means that the cooperative associations among lignin, PVP and surfactants are dominated by

**Table 2** Physicochemical properties and Williamson fitting parameters of 70:30 LSL/PVP solutions containing different types and concentrations of surfactants

Sample	$\eta_0$ (Pa·s)	$K$ ( $10^3$ ) (s)	$m$	Electrical conductivity ( $k$ ) ( $\mu\text{S}/\text{cm}$ )	Surface tension ( $\sigma$ ) (mN/m)
70:30 LSL:PVP (surfactant-free)	0.54	3.3	0.53	$470.7 \pm 1.9$	$36.91 \pm 0.04$
70:30 LSL:PVP+SDS					
0.01%	0.39	9.7	0.86	$777.3 \pm 3.5$	$35.13 \pm 0.12$
0.05%	0.88	4.1	0.54	$787.1 \pm 1.4$	$27.87 \pm 0.15$
0.1%	1.02	3.8	0.52	$801.3 \pm 7.1$	$24.36 \pm 0.11$
0.25%	1.29	5.3	0.51	$830.1 \pm 7.1$	$23.31 \pm 0.17$
0.5%	1.79	4.4	0.61	$850.1 \pm 1.2$	$23.88 \pm 0.05$
0.75%	2.15	5.4	0.73	$858.1 \pm 2.1$	$22.78 \pm 0.08$
1%	2.67	7.3	0.82	$919.2 \pm 4.1$	$22.71 \pm 0.03$
70:30 LSL:PVP+Tween-20					
0.01%	0.42	9.7	0.96	$499.1 \pm 2.1$	$35.48 \pm 0.07$
0.05%	0.95	2.9	0.64	$464.3 \pm 3.1$	$31.01 \pm 0.06$
0.1%	1.14	3.3	0.84	$438.1 \pm 3.1$	$25.63 \pm 0.09$
0.5%	1.44	4.4	0.77	$467.1 \pm 3.1$	$23.04 \pm 0.13$
1%	2.05	4.9	0.85	$482.7 \pm 0.6$	$22.27 \pm 0.11$
70:30 LSL:PVP+CTAB					
0.01%	0.38	9.9	0.95	$579.7 \pm 2.1$	$35.11 \pm 0.06$
0.05%	0.43	9.7	0.83	$671.3 \pm 4.5$	$30.79 \pm 0.09$
0.1%	0.98	2.8	0.73	$778.3 \pm 2.5$	$23.09 \pm 0.02$
0.5%	1.34	3.9	0.58	$841.3 \pm 2.1$	$20.55 \pm 0.12$
1%	1.88	7.1	0.67	$846.7 \pm 2.3$	$20.66 \pm 0.18$

the PVP-surfactant interactions [19]. The non-Newtonian flow response comprises almost constant values of viscosity over 2–3 decades and a subsequent shear-thinning region at relatively high shear rates, which can be described by the Williamson model, as shown for selected systems in Fig. 1. The corresponding fitting parameters for each solution are included in Table 2. A shear-thinning response was already evinced in the surfactant-free solution, thus PVP being the main responsible for the increased level of entanglements, which has been reported to be fundamental for the correct formation of fibers during the electrospinning [24, 28]. In general, the addition of surfactants may enhance, or not, the shear-thinning character of these complex solutions, depending on the predominant associations among the neutral polymer, lignin and the surfactant, as well as on surfactant concentration [22, 24]. In these systems, a small addition of surfactant, i.e. 0.01 wt. %, significantly enhanced the shear-thinning character (see higher values of parameter  $m$  in Table 2), suggesting the formation of new associations where the surfactants are involved. However, the addition of higher amounts of surfactants seems to dampen this effect but mainly to delay the onset

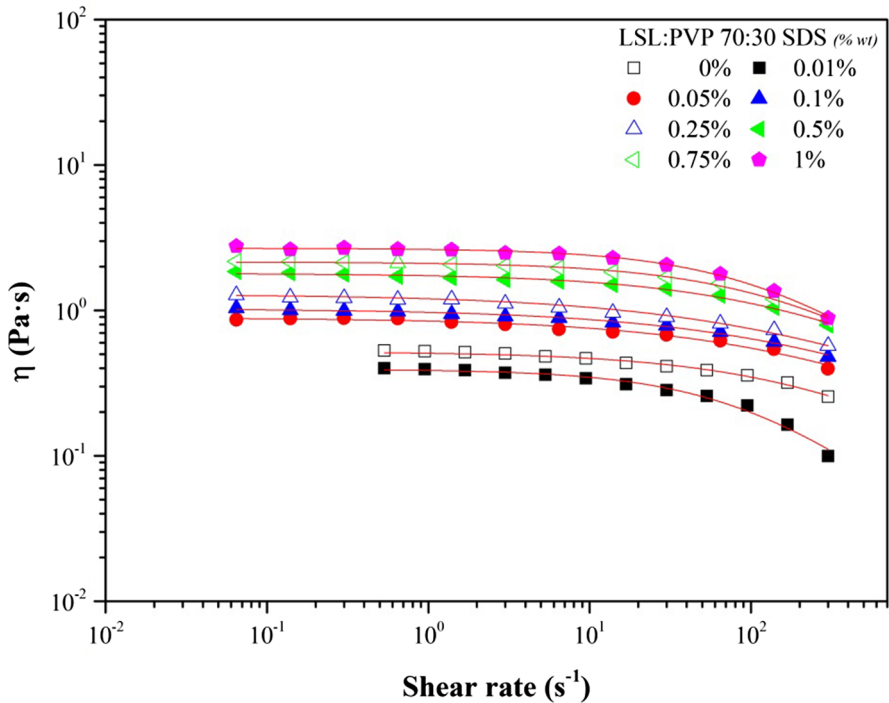


**Fig. 1** Viscous flow curves of LSL/PVP 70:30 solutions in DMF as a function of SDS concentration. Solid lines refer to the Williamson model fits (Eq. 1)

of shear thinning to higher shear rates (lower  $K$  values). More important, the values of the zero-shear-rate-limiting viscosity noticeably increased above a very low level of surfactant addition, i.e. 0.01 wt.%.

Apart from the impact on viscosity, surfactant addition influences other physicochemical properties of relevance for electrospinning such as electrical conductivity and surface tension. Surface tension and electrical conductivity values can be found in Tables 1 and 2 for all the LSL/PVP solutions studied. As expected, the addition of anionic and cationic surfactants significantly increased the electrical conductivity, yielding increments of around 90–100% with respect to the surfactant-free solutions when adding 1 wt.%. On the contrary, electrical conductivity is not much affected when adding the non-ionic surfactant (Tween-20). Moreover, as has been widely reported in the literature [21–25, 29], the addition of surfactants considerably decreases the surface tension of polymer solutions, with huge impact on the electrospinning process. This decrease in surface tension was especially relevant for the 70:30 LSL/PVP weight ratio, for which a reduction down to 20–23 mN/m was obtained. This means that the PVP-driven polymer–surfactant complexes have a superior surface activity than those dominated by LSL–surfactant interactions. In addition, the surface tension reduction was similar for all the surfactants studied although slightly larger for CTAB. The surface tension sharply decreased with a small addition



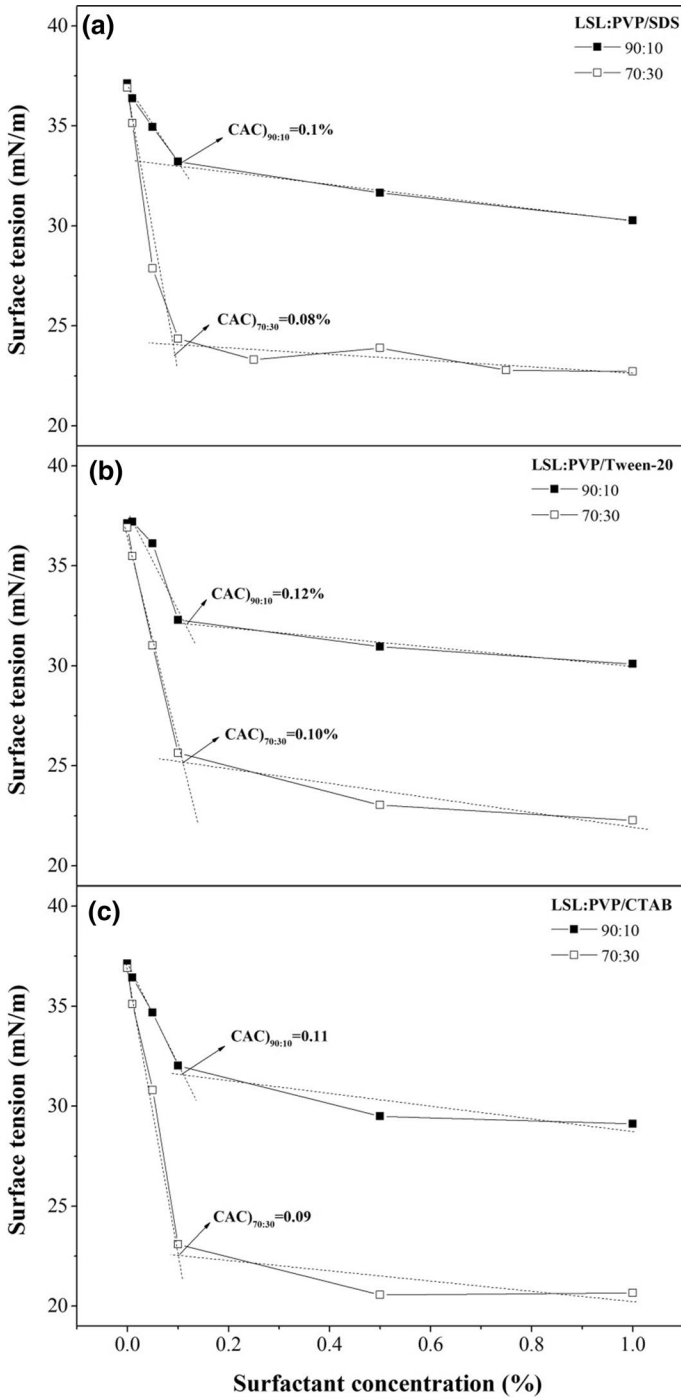


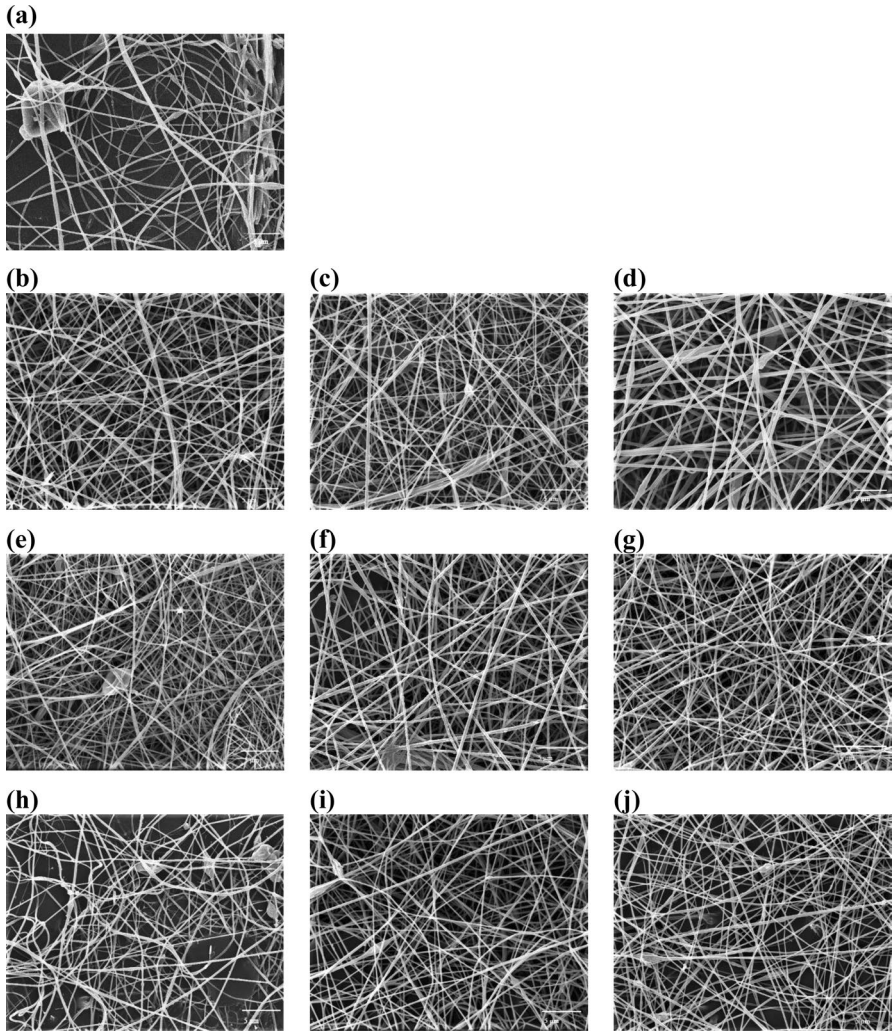
**Fig. 2** Evolution of surface tension with surfactant concentration and determination of the critical aggregation concentration (CAC) for **a** LSL/PVP/SDS **b** LSL/PVP/ Tween-20, and **c** LSL/ PVP/CTAB solutions

of surfactant and then reached an almost plateau value. This behavior is related to the presence and mobility of single surfactant molecules, and it is very well known for polymer-free surfactant solutions, where the surface tension significantly decreases up to reach the critical micelle concentration. In the case of polymer solutions, this plateau was reached earlier, at around CAC, when the surfactant mobility is reduced because of the polymer-surfactant interactions, as reported for PVP-surfactant solutions [19]. In fact, one of the methods proposed to determine the value of the critical aggregation concentration (CAC) is based on the variation of the surface tension with surfactant concentration [19, 30], as illustrated in Fig. 2. Thus, the CAC at which the polymer starts to interact with the surfactant determines the critical point for a reduction in surface activity. In the LSL/PVP solutions studied, the CAC is very similar for all the surfactants studied and varies between 0.08 and 0.12 wt.%. Slightly higher CACs than those obtained in this study for LSL-PVP-SDS solutions were reported for PVP-SDS solutions [19].

### **Effect of surfactant addition on the electrospinnability of LSL/PVP solutions and morphology of electrospun nanostructures**

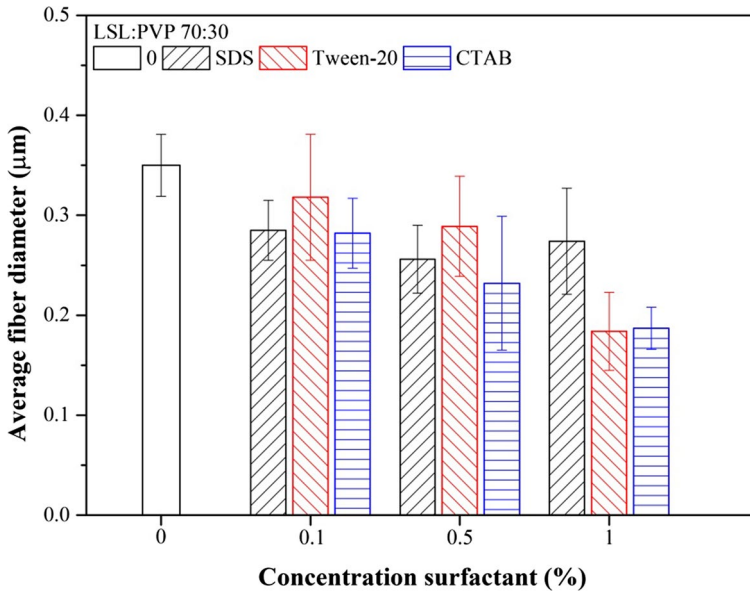
For a 70:30 LSL/PVP weight ratio, all the solutions were electrospinnable and nanofiber mats were obtained regardless of the type and concentration of surfactants, including the surfactant-free solution. This is due to a convenient combination of electrical conductivity, surface tension and rheological characteristics. As well known [31], both an increase in conductivity and a decrease in surface tension favor the stretching of nanofibers, whereas viscosity retards the stretching, thus reducing the filament rupture and/or increasing fiber diameter. On the other hand, a marked shear-thinning behavior favors filament stretching at high spinning flow rates and enhances jet formation.

As can be observed in Fig. 3, the addition of surfactant at concentrations around or above CAC produced more compact and uniform fiber mats with a higher amount of junctions and interconnected thin fibers due to improved electrospinnability, as a result of the increased level of entanglements in polymer solutions. However, the morphology of the nanofibers depends only slightly on the type and concentration of surfactant when added above this CAC. The presence of embedded particles and/or formation of large lumps eventually detected in nanofibers obtained from the surfactant-free solution (see Fig. 3a) were reduced with surfactant addition although not completely eliminated. Instead, morphologies very similar to those obtained from surfactant-free solutions were found at surfactant concentrations below CAC (results not shown). Moreover, typical beads appearing in lignin nanofibers [32] are scarcely present when adding surfactants and tend to disappear at high SDS and Tween-20 concentrations. However, some beaded nanofibers are apparent when adding CTAB, even at 1 wt.% (Fig. 3j). This fact can be explained on the basis of the more favorable interaction between CTAB and lignin, excluding PVP to some extent from the complexes, which also is associated to a lower shear-thinning character in comparison with SDS and Tween-20 (see *m* values in Table 2). On the other hand, thicker fibers and/or bundles



**Fig. 3** SEM Images of 70:30 LSL/PVP nanofibers mats obtained with different types and concentrations of surfactants: **a** surfactant-free, **b** 0.1 wt.% SDS, **c** 0.5 wt.% SDS, **d** 1 wt.% SDS, **e** 0.1 wt.% Tween-20, **f** 0.5 wt.% Tween-20, **g** 1 wt.% Tween-20, **h** 0.1 wt.% CTAB, **i** 0.5 wt.% CTAB and **j** 1 wt.% CTAB. (Magnification 4000x, scale bars correspond to 5  $\mu$ m)

of fibers were found in nanofiber mats containing 1 wt.% SDS (see Fig. 3d), which may be related to the particularly high viscosity of the spinning solution (see Table 2). In contrast, highly homogeneous and almost bead-free thin fiber mats were especially obtained from solutions containing high contents of Tween-20 (see Fig. 3g). This fact suggests that surfactant-polymer complexes favored by ionic surfactants cause a certain degree of agglomeration producing beaded fibers and/or bundles to some extent. Average fiber diameter generally decreased with surfactant concentration, as shown in



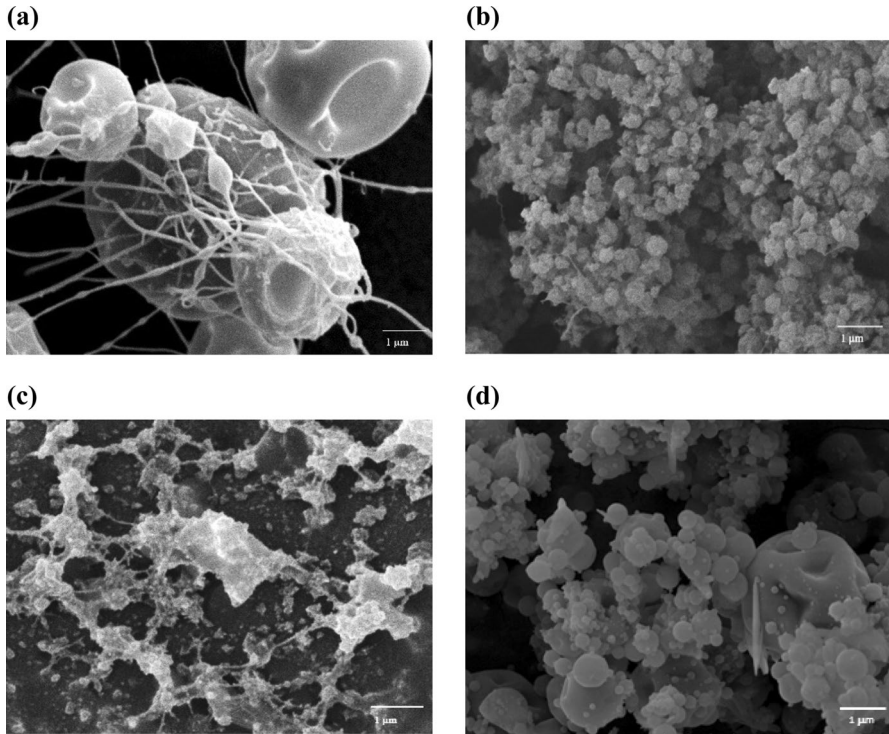
**Fig. 4** Average fiber diameter of LSL/PVP 70:30 solutions containing different types and concentrations of surfactants

Fig. 4. This phenomenon is mainly due to the surfactant-induced reduction in surface tension and enhanced shear-thinning character, making easier the stretching of the jet in the Taylor cone, and has been widely reported for instance for PVP, PVA and lignin/PVA nanofibers [21, 25, 33]. Fiber diameter was especially reduced by adding 1 wt.% Tween-20 or CTAB to the electrospun LSL/PVP solution. In contrast, as discussed above, the more entangled LSL-PVP-SDS complexes generally imparting higher viscosity to the solution seem to promote the formation of thicker fibers or fiber bundles, slightly increasing the average fiber diameter at high SDS concentration.

For a higher LSL/PVP weight ratio, i.e. 90:10, nanofibers were not obtained but electrospayed particles connected by thin filaments, probably as a result of not high enough levels of entanglements in the polymeric solutions. Moreover, the addition of surfactant is not advantageous for obtaining fibers, although some unusual nanostructures were produced, and particle size was significantly reduced. As can be seen in Fig. 5, the addition of small amounts of SDS or CTAB leads to the appearance of uniform structures composed of clusters of small (nanosized) particles. In the particular case of Tween-20, some networks of such small particles and agglomerates are apparent.

### Oil structuring ability

The different electrospun nanostructures obtained from LSL/PVP/surfactant solutions were mixed with castor oil, at 20% wt. concentration, to examine the ability



**Fig. 5** SEM Images of 90:10 LSL/PVP nanostructures obtained with different types of surfactants: **a** surfactant-free, **b** 0.1 wt.% SDS, **c** 0.1 wt.% Tween-20 and **d** 0.1 wt.% CTAB. (Magnification 10,000x, scale bars correspond to 1 μm)

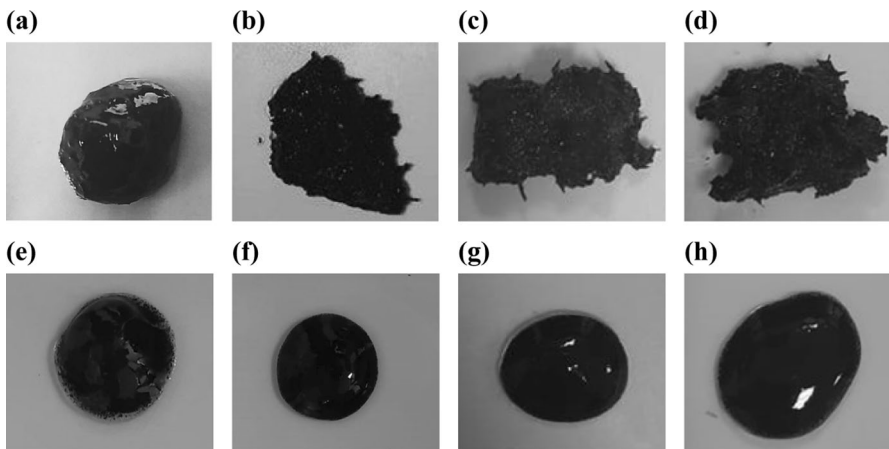


**Fig. 6** Blends of castor oil and LSL/PVP nanostructures at 20 wt.% concentration. Upper row, 70:30 LSL/PVP nanofibers, **a** surfactant-free, **b** 0.5 wt.% SDS, **c** 0.5 wt.% Tween-20 and **d** 0.5 wt.% CTAB. Lower row, 90:10 LSL/PVP nanostructures, **e** surfactant-free, **f** 0.5 wt.% SDS, **g** 0.5 wt.% Tween-20 and **h** 0.5 wt.% CTAB

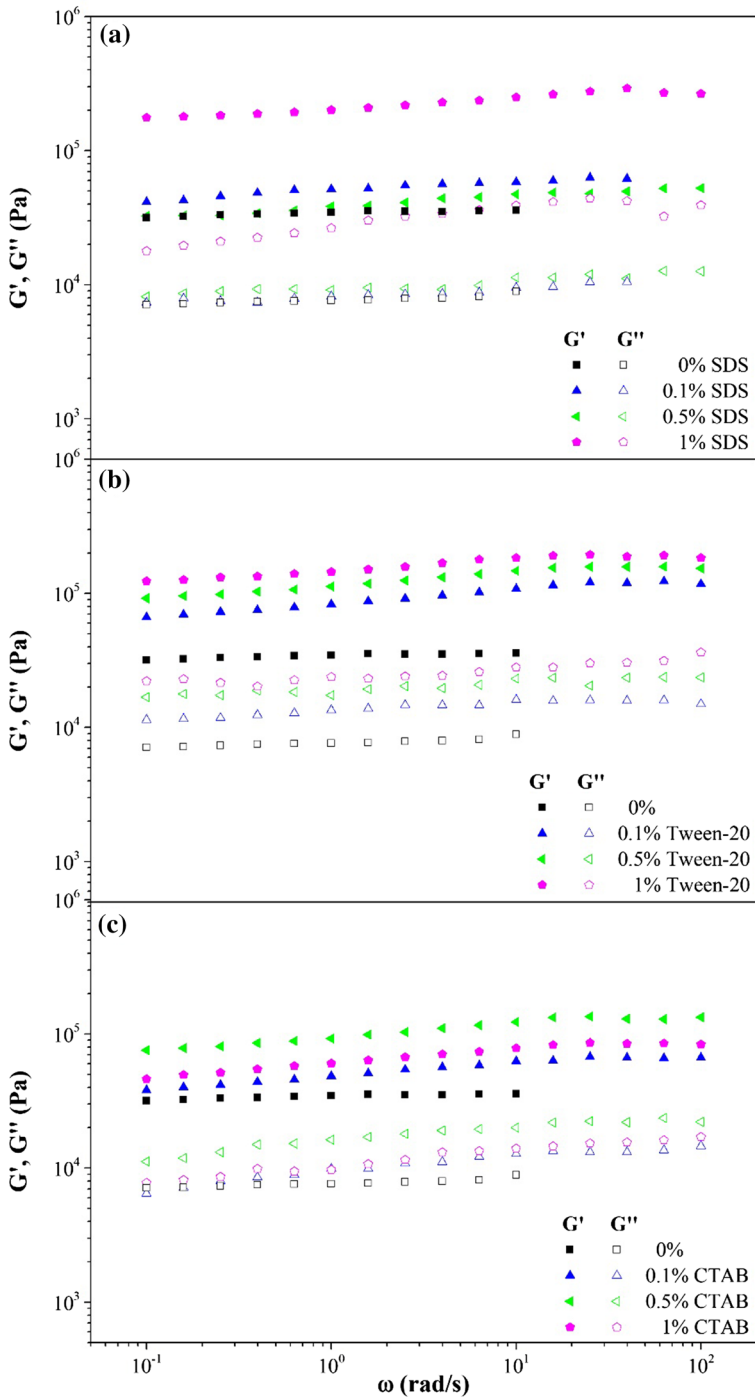
**Fig. 7** Evolution of linear viscoelastic functions with frequency for oleogels prepared with 20 wt.% of 70:30 LSL/PVP electrospun nanofibers by adding **a** SDS, **b** Tween-20 and **c** CTAB surfactants at different concentration

to form oleogels. As can be observed in Fig. 6, nanofiber mats obtained by electrospinning from 70:30 LSL/PVP solutions were able to generate physically stable and though oleogels (Fig. 6a–d). However, the nanostructures obtained upon addition of surfactants (SDS, Tween-20 or CTAB) to a 90:10 LSL/PVP solution promote the formation of apparently thickened liquids or soft gels (see Fig. 6f–h), whereas the nanostructure obtained from the surfactant-free solution yields an unstable dispersion where a certain degree of separation can be appreciated (see Fig. 6e). In general, the formation of well-developed nanofiber mats, regardless the presence of beads or bundles, was required to noticeably structure oil. As previously reported [18], nanofiber mats are able to entrap castor oil more favorably in the porous network, thus enhancing the physical interactions between the oil and the LSL/PVP fibers. Figure 7 shows the influence of surfactant concentration on the rheological response of oleogels prepared with 70:30 LSL/PVP nanofibers. The evolution of the storage ( $G'$ ) and loss ( $G''$ ) functions with frequency is concordant with the definition given by Almdal et al. [34] for solid-like gels and qualitatively similar in all cases. Differences of around one decade between both SAOS functions can be observed as well as small slopes of the  $G'$  and  $G''$  vs. frequency plots. In contrast, gels prepared by dispersing 90:10 LSL/PVP nanofibers in castor oil exhibited rheological characteristics of soft gels (Fig. 8), with values of  $G'$  and  $G''$  much lower to those shown in Fig. 7 and a tendency to crossover at high frequencies.

The values of the viscoelastic functions increased with surfactant addition. However, as can be seen in Fig. 7, nanofibers obtained from the surfactant-free solution provided values of both SAOS functions similar to those found for oleogels prepared with nanostructures resulting from solutions having small concentration of ionic surfactants (SDS and CTAB), i.e. around the CAC, whereas higher surfactant concentrations generally produced noticeable increments in the viscoelastic functions. Overall, higher values of SAOS functions correspond to oleogels stabilized with more uniform and compact nanofiber mats, like those obtained with Tween-20. Again, the fiber membrane obtained from the LSL/PVP solution containing 1 wt.% SDS showed a distinctive behavior, providing the oleogel with the highest viscoelastic functions, despite showing a higher average fiber diameter (see Fig. 4). On the contrary, the nanofiber templates obtained from solutions containing CTAB, which evinced some beaded fibers, generally displayed low values of the viscoelastic functions, particularly that prepared from the solution having 1 wt.% CTAB.

### Tribological performance of oleogels structured with LSL/PVP nanofiber mats

To explore a potential lubricant application of these oleogels, the tribological performance was assessed in a ball-on-three-plate steel–steel tribological contact [27]. Figure 9 collects the friction coefficient values and average diameter of the resulting wear scars generated on the plates. As can be seen, all the oleogels



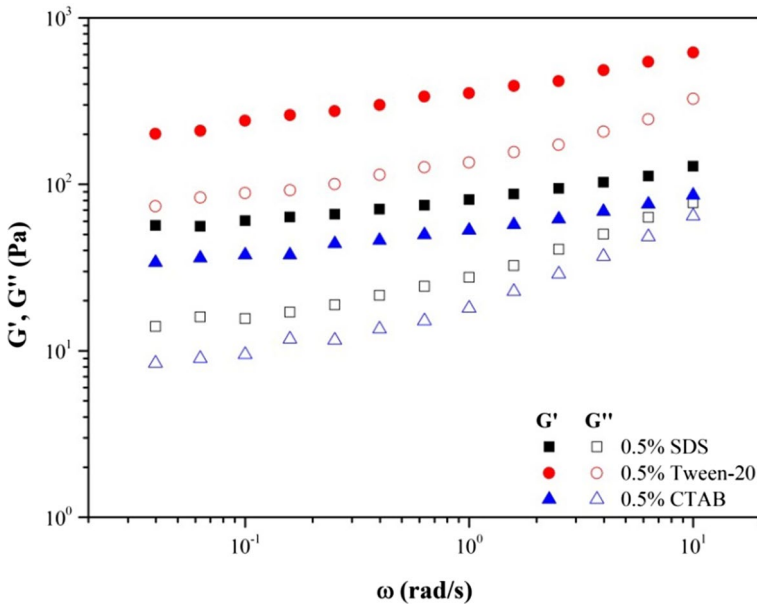


**Fig. 8** Evolution of linear viscoelastic functions with frequency for oleogels prepared with 20 wt.% of 90:10 LSL/PVP electrospun nanostructures by adding 0.5% wt. surfactant

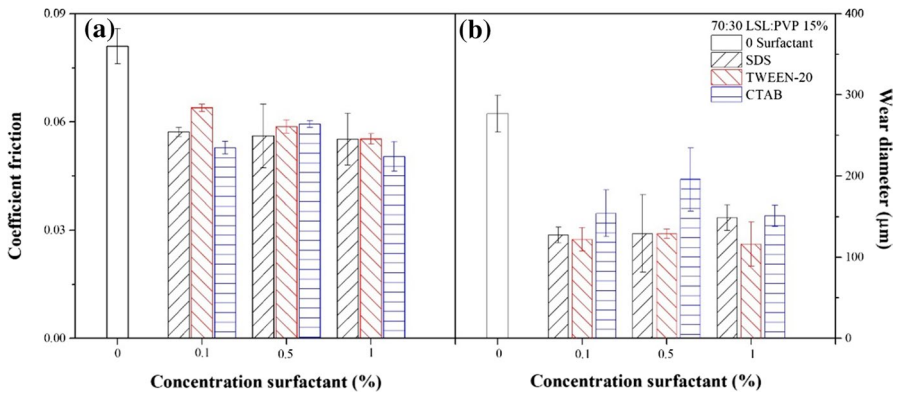


**Fig. 9** Friction coefficient (a) and wear scar diameters (b), as a function of surfactant concentration, resulting when 70:30 LSL/PVP nanofiber-based oleogels were applied as lubricants in a tribological contact

prepared with nanofiber mats obtained by electrospinning from 70:30 LSL/PVP solutions containing surfactants provided excellent lubrication performance, with



extremely low values of the friction coefficient and wear scar diameters, generally much lower than those found when using conventional lubricating greases [35, 36] or chemically functionalized cellulose- and lignin-based oleogels [13, 36, 37] under similar conditions (i.e. friction coefficient values typically ranging from 0.07 to 0.12). Moreover, the addition of surfactants to the electrospun solution is beneficial since significantly lower values of both friction coefficient and wear scar diameters were obtained in comparison with those generated when using the oleogel prepared with the surfactant-free membrane. This result supports the idea that well-developed and more uniform nanofiber mats allow the oleogel to penetrate into the lubricating contact as a whole, promoting oil release once the nanostructure is stressed [18], at the same time that nanofibers may also prevent wear by increasing the film thickness. Regarding the kind of surfactant, no significant differences were found in the friction coefficient, but slightly larger wear scars were obtained when adding CTAB. These results are in agreement with the general opinion [38] that surfactants enhance the film formation of lubricants in a tribological contact, therefore imparting anti-wear properties.

## Conclusions

Different nanostructures were produced by electrospinning from solutions of low-sulfonate lignin (LSL) and polyvinylpyrrolidone (PVP) in DMF, prepared at two different LSL/PVP weight ratios, 70:30 and 90:10, by adding variable concentrations (0–1 wt.%) of anionic (SDS), cationic (CTAB) and non-ionic (Tween-20) surfactants. 90:10 LSL/PVP solutions are Newtonian and the viscosity initially decreased with surfactant addition and then increased from a critical concentration in the case of ionic surfactants (SDS and CTAB), while viscosity slightly decreased initially and remained almost constant when adding the non-ionic surfactant (Tween-20). This behavior has been explained on the basis of different electrical and hydrophobic surfactant-lignin and surfactant-PVP interactions. In general, the increase in viscosity is especially favored by the formation of surfactant-polymer complexes above the critical aggregation concentration (CAC), which determines the onset of surfactant-polymer interaction. CAC was determined through the variation of the surface tension with surfactant concentration being very similar for all the surfactants studied, ranging from 0.08 to 0.12 wt.% For a 70:30 LSL/PVP weight ratio, solutions showed a non-Newtonian flow response and the viscosity always increased with surfactant concentration above 0.01 wt%, regardless of the type of surfactant, suggesting that the cooperative associations among lignin, PVP and surfactant are dominated by the PVP-surfactant interactions.

The addition of surfactants to 70:30 LSL/PVP solutions yields more compact and uniform fiber mats with a higher amount of junctions and generally reducing the average diameter of the nanofibers and the number of beads. However, beaded fibers are apparent when adding CTAB, even at 1 wt.%, whereas thick fibers and/or bundles of fibers were found in nanofiber mats containing 1 wt.% SDS. This fact suggests that surfactant-polymer complexes favored by ionic surfactants

cause a certain degree of agglomeration to some extent producing beaded fibers and/or bundles. In contrast, highly homogeneous and almost bead-free fiber mats were obtained from solutions containing high contents of Tween-20. On the other hand, nanofiber mats were not obtained with 90:10 LSL/PVP solutions but different nanostructures composed of electrosprayed particles eventually connected by thin filaments or particle clusters.

Nanostructures obtained upon addition of surfactants (SDS, Tween-20 or CTAB) to a 90:10 LSL/PVP solutions were able to form soft gels with the appearance of thickened liquids, while nanofiber mats obtained by electrospinning from 70:30 LSL/PVP solutions generated strong oleogels at 20% wt. concentration. In general, SAOS viscoelastic functions slightly increased with the surfactant concentration. In addition, these oleogels also showed excellent lubrication performance in a tribological contact, yielding extremely low values of the friction coefficient and wear, generally much lower than those found when using conventional lubricating greases. Moreover, the addition of surfactants to the electrospun solution significantly lowers both friction and wear in comparison with the oleogel prepared with surfactant-free nanofiber mats.

Overall, the addition of small amounts of surfactant to LSL/PVP solutions improves electrospinnability as well as the ability of resulting nanofiber mats to structure castor oil, resulting oleogels with enhanced rheological and tribological properties, which can drive potential applications as lubricants.

**Acknowledgements** This work is part of a research project (RTI2018-096080-B-C21) funded by MCIN/AEI/10.13039/501100011033 and by “ERDF A way of making Europe.” The financial support is gratefully acknowledged.

**Funding** Open Access funding provided by Universidad de Huelva / CBUA, thanks to the CRUE-CSIC agreement with Springer Nature.

## Declarations

**Conflict of interest** The authors declare that there is no actual or potential conflict of interest in relation to this article.

**Open Access** This article is licensed under a Creative Commons Attribution 4.0 International License, which permits use, sharing, adaptation, distribution and reproduction in any medium or format, as long as you give appropriate credit to the original author(s) and the source, provide a link to the Creative Commons licence, and indicate if changes were made. The images or other third party material in this article are included in the article’s Creative Commons licence, unless indicated otherwise in a credit line to the material. If material is not included in the article’s Creative Commons licence and your intended use is not permitted by statutory regulation or exceeds the permitted use, you will need to obtain permission directly from the copyright holder. To view a copy of this licence, visit <http://creativecommons.org/licenses/by/4.0/>.

## References

1. Soni S, Agarwal M (2014) Lubricants from renewable energy sources—a review. *Green Chem Lett Rev* 7(4):359–382

2. Sadh PK, Duhan S, Duhan JS (2018) Agro-industrial wastes and their utilization using solid state fermentation: a review. *Bioresour Bioprocess* 5(1):1–15
3. Dachowski R, Kostrzewa P (2016) The use of waste materials in the construction industry. *Procedia Eng* 161:754–758
4. Kwek SY, Awang H (2021) Utilization of industrial waste materials for the production of light-weight aggregates: a review. *J Sustain Cem Mater* 10(6):353–381
5. Panchal TM, Patel A, Chauhan DD, Thomas M, Patel JV (2017) A methodological review on bio-lubricants from vegetable oil based resources. *Renew Sustain Energy Rev* 70:65–70
6. Carvajal JC, Gómez Á, Cardona CA (2016) Comparison of lignin extraction processes: economic and environmental assessment. *Bioresour Technol* 214:468–476
7. Pelaez-Samaniego MR, Yadama V, Garcia-Perez M, Lowell E, Zhu R, Englund K (2016) Inter-relationship between lignin-rich dichloromethane extracts of hot water-treated wood fibers and high-density polyethylene (HDPE) in wood plastic composite (WPC) production. *Holzforschung* 70(1):31–38
8. Thakur VK, Thakur MK (2015) Recent advances in green hydrogels from lignin: a review. *Int J Biol Macromol* 72:834–347
9. Ragauskas AJ, Beckham GT, Bidy MJ, Chandra R, Chen F, Davis MF, Davison BH, Dixon RA 4, Gilna P, Keller M, Langan P, Naskar AK, Saddler JN, Tschaplinski TJ, Tuskan GA, Wyman CE (2014) Lignin valorization: improving lignin processing in the biorefinery. *Science* 344: 6185
10. Cecutti C, Agius D (2008) Ecotoxicity and biodegradability in soil and aqueous media of lubricants used in forestry applications. *Bioresour Technol* 99(17):8492–8496
11. Núñez N, Martín-Alfonso JE, Valencia C, Sánchez MC, Franco JM (2012) Rheology of new green lubricating grease formulations containing cellulose pulp and its methylated derivative as thickener agents. *Ind Crops Prod* 37(1):500–507
12. Gallego R, Arteaga JF, Valencia C, Díaz MJ, Franco JM (2015) Gel-like dispersions of hmdi-cross-linked lignocellulosic materials in castor oil: toward completely renewable lubricating grease formulations. *ACS Sustain Chem Eng* 3(9):2130–2141
13. Delgado MA, Cortés-Triviño E, Valencia C, Franco JM (2020) Tribological study of epoxide-functionalized alkali lignin-based gel-like biogreases. *Tribol Int* 146:106231
14. Cortés-Triviño E, Valencia C, Franco JM (2017) Influence of epoxidation conditions on the rheological properties of gel-like dispersions of epoxidized kraft lignin in castor oil. *Holzforschung* 71(10):777–784
15. Borrero-López AM, Martín-Sampedro R, Ibarra D, Valencia C, Eugenio ME, Franco JM (2020) Evaluation of lignin-enriched side-streams from different biomass conversion processes as thickeners in bio-lubricant formulations. *Int J Biol Macromol* 162:1398–1413
16. Borrero-López AM, Blánquez A, Valencia C, Hernández M, Arias ME, Eugenio ME, Fillat U, Franco JM (2018) Valorization of soda lignin from wheat straw solid-state fermentation: production of oleogels. *ACS Sustain Chem Eng* 6(4):5198–5205
17. Borrero-López AM, Blánquez A, Valencia C, Hernández M, Arias ME, Franco JM (2019) Influence of solid-state fermentation with *Streptomyces* on the ability of wheat and barley straws to thicken castor oil for lubricating purposes. *Ind Crops Prod* 140:111625
18. Borrego M, Martín-Alfonso JE, Sánchez MC, Valencia C, Franco JM (2021) Electrospun lignin-PVP nanofibers and their ability for structuring oil. *Int J Biol Macromol* 180:212–221
19. Kumar N, Tyagi R (2015) Analysis of the interactions of *Polyvinylpyrrolidone* with conventional anionic and dimeric anionic surfactant. *J Dispers Sci Technol* 36(11):1601–1606
20. Wang SC, Wei TC, Bin CW, Tsao HK (2004) Effects of surfactant micelles on viscosity and conductivity of poly(ethylene glycol) solutions. *J Chem Phys* 120(10):4980–4988
21. Jia L, Qin XH (2013) The effect of different surfactants on the electrospinning poly(vinyl alcohol) (PVA) nanofibers. *J Therm Anal Calorim* 112(2):595–605
22. Fang W, Yang S, Yuan TQ, Charlton A, Sun RC (2017) Effects of various surfactants on alkali lignin electrospinning ability and spun fibers. *Ind Eng Chem Res* 56(34):9551–9559
23. Araújo ES, Nascimento MLF, de Oliveira HP (2013) Influence of triton X-100 on PVA fibres production by the electrospinning technique. *Fibres Text East Eur* 100(4):39–43
24. Kriegel C, Kit KM, McClements DJ, Weiss J (2009) Electrospinning of chitosan-poly(ethylene oxide) blend nanofibers in the presence of micellar surfactant solutions. *Polymer* 50(1):189–200
25. Wang S-Q, He J-H, Xu L (2008) Non-ionic surfactants for enhancing electrospinnability and for the preparation of electrospun nanofibers. *Polym Int* 57:1079–1082

26. Quinchia LA, Delgado MA, Franco JM, Spikes HA, Gallegos C (2012) Low-temperature flow behaviour of vegetable oil-based lubricants. *Ind Crops Prod* 37(1):383–388
27. Heyer P, Luger J (2009) Correlation between friction and flow of lubricating greases in a new tribometer device. *Lubr Sci* 21(6):253–268
28. Wongsasulak S, Kit KM, McClements DJ, Yoovidhya T, Weiss J (2007) The effect of solution properties on the morphology of ultrafine electrospun egg albumen–PEO composite fibers. *Polymer* 48(2):448–457
29. Chari K, Antalek B, Lin MY, Sinha SK (1994) The viscosity of polymer-surfactant mixtures in water. *J Chem Phys* 100(7):5294–5300
30. Holmberg K, Jonsson B, Kronberg B, Lindman B (2003) *Surfactants and polymers in aqueous solution*. Wiley, New York, pp 39–66
31. Kriegel C, Arrechi A, Kit K, McClements DJ, Weiss J (2008) Fabrication, functionalization, and application of electrospun biopolymer nanofibers. *Crit Rev Food Sci Nutr* 48(8):775–797
32. Dallmeyer I, Ko F, Kadla JF (2010) Electrospinning of technical lignins for the production of fibrous networks. *J Wood Chem Technol* 30(4):315–329
33. Dallmeyer I, Ko F, Kadla JF (2014) Correlation of elongational fluid properties to fiber diameter in electrospinning of softwood kraft lignin solutions. *Ind Eng Chem Res* 53(7):2697–2705
34. Almdal K, Dyre J, Hvidt S, Kramer O (1993) Towards a phenomenological definition of the term “gel.” *Polym Gels Networks* 1(1):5–17
35. Sanchez R, Valencia C, Franco JM (2014) Rheological and tribological characterization of a new acylated chitosan-based biodegradable lubricating grease: a comparative study with traditional lithium and calcium greases. *Tribol Trans* 57(3):445–454
36. Gallego R, Cidade T, Sanchez R, Valencia C, Franco JM (2016) Tribological behaviour of novel chemically modified biopolymer-thickened lubricating greases investigated in a steel-steel rotating ball-on-three plates tribology cell. *Tribol Int* 94:652–660
37. Cortes-Trivino E, Valencia C, Delgado MA, Franco JM (2019) Thermo-rheological and tribological properties of novel bio-lubricating greases thickened with epoxidized lignocellulosic materials. *J Ind Eng Chem* 80:626–632
38. Pogosian AK, Martirosyan TR (2007) Impact of surfactant structure on the tribological properties of bentonite-based greases. *J Tribol* 129(4):920–922

**Publisher's Note** Springer Nature remains neutral with regard to jurisdictional claims in published maps and institutional affiliations.